J. Membrane Biol. 3, 291 – 312 (1970)

Electrical Characteristics of the Ionic psn-Junction as a Model of the Resting Axon Membrane*

GEROLD ADAM

Fachbereich Chemie, Universität Konstanz, Konstanz, Germany

Received 9 April 1970

Summary. As a model for the resting axon membrane, we propose the ionic psn-junction. Its electrical characteristics can be determined in close analogy to the corresponding electronic semiconductor junction. Using the "semianalytic approximation", we calculated the electrical capacity and the ionic currents. In contrast to the abrupt pn-junction, the electrical capacity of the psn-junction turns out to be practically voltage-independent, as it is observed for the squid axon membrane. The passive ionic fluxes for K^+, Na^+ and Cl^-, as the main contributions to the total charge flux, are calculated and compared with literature data on the ion fluxes through the resting squid axon membrane as measured by use of radioactive tracers. From this comparison, the ionic permeabilities can be evaluated and used to compute the resting membrane conductivity, which is found to be close to the experimental value. Further evidence in favor of the proposed asymmetrical membrane structure and possible ways of its test by the methods of protein chemistry are discussed.

An interesting class of theoretical models for biological membranes was proposed by Mauro (1962) and Coster (1965). These authors considered the ionic pn-junction as a basic structure of biological membranes and derived its electrical characteristics in close analogy to those of the electronic pn-junction of semiconductor physics.

Mauro (1962) was able to show that the ionic pn-junction exhibits an electrical capacitance of the order of magnitude found for the membranes of numerous different types of cells. Coster (1965), using certain approximations, was able to calculate the nonlinear steady state conductivity of the ionic pn-junction, which for reasonable choices of parameters compared well with that of giant marine algae. Subsequently, in an important paper, Coster, George and Simons (1969), by numerical integration of the Nernst-

* Part of this work was carried out at the Institut für Physiologische Chemie, Universität München, during the tenure of a Habilitandenstipendium of the Deutsche Forschungsgemeinschaft.

Planck equations of the pn-junction, verified the validity of the approx mations made by Coster (1965).

As a modification of the model of Mauro and Coster, we have propose the ionic psn-junction as a model for the squid axon membrane (Adam 1967, 1968, 1970). In the present paper, we give in some detail calculation of steady state electrical characteristics of the psn-junction which diffe qualitatively from those of the pn-junction. The theoretical results ar compared with experimental data taken from the literature on electrica capacity, ionic fluxes and electrical conductivity of the squid axon membran in the resting state.

Fixed-Charge Model of the Membrane

Our proposed model of the axon membrane (Adam, 1967, 1968, 1970 augments the pn-junction of Mauro (1962) and Coster (1965) by a centra s-layer. This structure is analogous to the electronic psn-junction in elec tronic semiconductor devices (Herlet & Spenke, 1965).

We were led to this modification by the numerous results from electron microscopic and X-ray investigations of biological membranes, which show a three-layered structure. High-resolution electron micrographs for the squid giant axolemma were published recently (Villegas & Villegas, 1968) and exhibit the familar three-layered structure. An extensive review on the structural, chemical and electrical data of biological membranes was given by Stoeckenius and Engelman (1969). These data seem to be in accord with the membrane model of Davson and Danielli (1952). According to Davson and Danielli, biological membranes consist of two protein layers, facing the electrolyte reservoirs on both sides of the membrane and sandwiching a phospholipid bilayer.

Correspondingly, we consider the axolemma as a three-layered structure (*see* Fig. 1).

The n-layer, facing the extracellular compartment, is considered to have an excess of fixed positively charged groups. Thus, the mobile majority charge carriers are anions. The effective dielectric constant of the n-layer is ε_n. Conversely, the p-layer faces the intracellular compartment and has an excess of fixed negatively charged groups in a milieu of an effective dielectric constant ε_p. The central s-layer of dielectric constant ε_s has only few fixed charges, which in first approximation can be neglected in comparison to those of the n- and p-layers. To account for transport of water-soluble metabolites and ions through the membrane, either pores of molecular dimensions or mobile carriers have been postulated. For the purposes

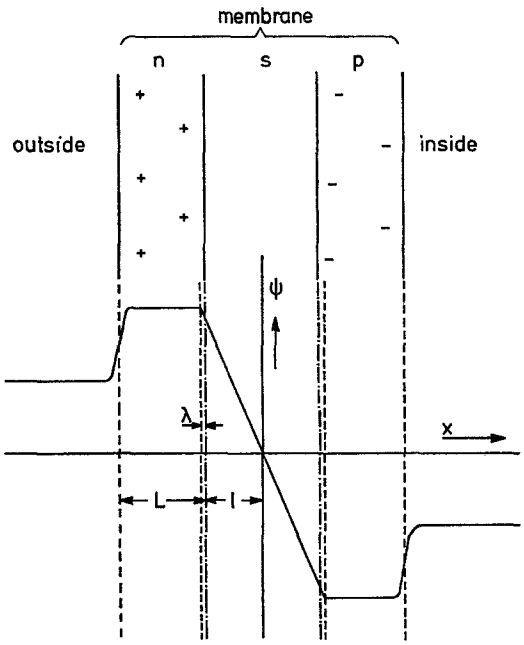

Fig. 1. Schematic representation of the membrane model (above) and of the profile of the electric potential (below)

of the present paper, we need not specify which of the two possibilites of transit of solutes through the s-layer occurs in our model, but only that one does exist.

Since we are interested solely in the general properties of the psn-junction, we consider only the symmetrical case where the excess concentration N_+ of positively charged fixed groups in the n-layer is equal to the excess concentration N_- of negatively charged fixed groups in the p-layer:

$$N_+ = N_- = N \tag{1}$$

and furthermore:

$$\varepsilon_n = \varepsilon_p = \varepsilon\,. \tag{2}$$

Although our model is fairly general, for a more vivid physical ficture it seems useful to give some numerical estimates of its parameters. If we interpret our model in terms of the Davson-Danielli model, the n- and p-layers are composed of membrane-bound hydrophilic proteins and of the hydrophilic groups of the phospholipids. The s-layer can be thought of as composed of the hydrophobic hydrocarbon chains of the phospholipids

and of the mobile carrier molecules or the pores having a hydrophilic interior.

Thus, we expect the effective dielectric constant of the p- and n-layer to be of the order of magnitude encountered in ion-exchange resins, where there is a volume fraction, of say 0.5, of organic phase distributed in a watery phase. According to the estimates of Rice and Nagasawa (1961, p. 470), we thus expect $\varepsilon = 30$ to 40 ε_0, where $\varepsilon_0 = 8.86 \cdot 10^{-14}$ coul V^{-1} cm^{-1}. By a similar argument, the effective dielectric constant of the s-layer with predominantly hydrocarbon chains of phospholipids is estimated to be about $\varepsilon_s = 4\,\varepsilon_0$. Not much is known about the number of fixed charged groups on either side of a biological membrane. An estimate can be derived from the membrane-bound mitochondrial protein cytochrome *c*. It carries an excess of eight positively charged groups (Margoliash, 1962) in a volume of $25 \times 25 \times 37$ A^3 (Dickerson, Kopka, Weinzierl, Varnum, Eisenberg & Margoliash, 1967), giving a mean concentration of $N_+ = 0.6$ M. Another estimate comes from the basic polypeptide protamine, which by Mueller and Rudin (1967, 1968*a*, *b*) was adsorbed to lipid bilayer membranes and gave rise to action potentials. Protamines are of molecular weight 1,000 to 5,000. They contain predominantly arginine; for instance, clupein has 22 molecules of arginine and only 11 molecules of other amino acids, giving an excess of at least 11 positively charged groups per molecule (Karlson, 1966, p. 34). Using a protein density of $\rho = 1.25$ g/cm^3 and a molecular weight of 5,000, we obtain for clupein $N_+ \geqq 2.6$ M.

Thus, we can expect net concentrations of $N_+ = 1$ to 5 M of fixed charged groups in densely packed n-layers of such proteins. Similar values are reasonable for the p-layer of our model. A distribution of fixed charges as proposed in our psn-model gives rise to a distribution of the electrical potential as shown schematically in Fig. 1. A more detailed discussion of the potential distribution will be given in later sections. At this place we give only some numbers of the magnitudes to be expected. For the squid giant axon in the physiological state, the concentration of univalent 1:1 electrolyte in the extra- and intracellular compartment is about 0.5 M. For a fixed-charge lattice of $N_+ = 1$, 2, and 5 M, the Donnan potential between the extracellular medium and the interior of the n-layer is 21, 36, and 58 mV, respectively. Here, a partition coefficient of one was used. The total drop of electrical potential across the s-layer is the sum of the two Donnan potentials and the resting potential. With a resting potential of about -60 mV, as encountered for the squid giant axon of different species, we get for a membrane with $N_+ = N_- = 2$ M a potential drop across the s-layer of 132 mV in the resting state. Finally, we wish to assign tentative numbers

to the thicknesses of the n-, p-, and s-layers. The s-layer is supposed to be about 40 A thick, corresponding to twice the length of an extended hydrocarbon chain of a phospholipid molecule. The n- and p-layers will be about 30 A thick, which then gives for their average distance about 70 A, as observed electron microscopically for most biological membranes.

Semianalytic Approximation

For a straightforward integration of the Nernst-Planck equation of the ionic psn-junction, one has to use numerical procedures. As shown by Coster *et al.* (1969) for the pn-junction, such a computer solution proves to be very time-consuming and costly. Thus, we shall use in the following calculations the semianalytic procedure introduced by Coster (1965). The assumptions of this procedure in terms of our model are the following (*see* also Coster *et al.*, 1969):

(1) In moving from the solution phase into the p- or n-layer, the profiles of electric potential and ion concentrations reach steady levels at distances which are small compared to the width of the p- and n-layers.

Estimates on the validity of this assumption have been made by Mauro (1962). In the absence of more detailed information, one uses for estimates of this kind the presumptions of a partition coefficient between electrolyte solution and a fixed-charge lattice of one and of an activity coefficient of one. The further approximation $N_+ \gg c$, of Mauro (1962), where c is the electrolyte concentration in the solution phase, is not applicable to our system. In our case, we have $N_+ \sim 1$ to 5 M and $c \sim 0.5$ M. Therefore, we have checked the above assumption (1) by numerical integration of Eq. (18) of Mauro's paper (1962). The result is shown in Fig. 2, where we have plotted the normalized rise of the electrical potential ψ in dependence of the distance from the fixed-charge lattice-solution boundary. Here ψ_0 is the electrical potential at this boundary and ψ_∞ the steady level of electrical potential far in the fixed-charge lattice. As can be seen from this diagram, the above assumption (1) is valid; the electrical potential rises to its steady level within a few Angstrom. Mauro (1962) has shown that not all of the Donnan-potential step occurs within the fixed-charge lattice. For completeness, we have assembled in Table 1 the Donnan potential ψ_D, the potential rise $(\psi_\infty - \psi_0)$ within the fixed-charge lattice, and the distance d in A, in which the potential rise in the fixed-charge lattice is completed up to $1/e$. The numbers in Table 1 correspond to the parameters $N_+/2c$ used in Fig. 1.

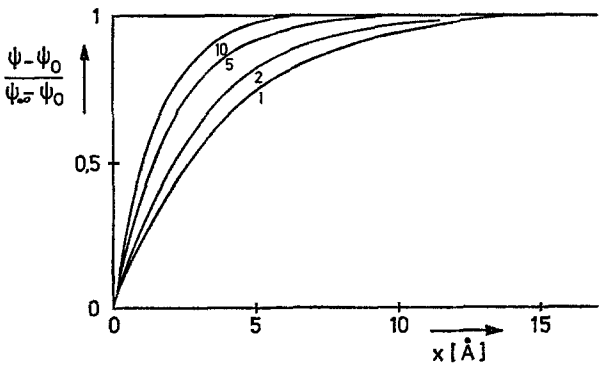

Fig. 2. Normalized profile of the electric potential inside of the n-layer, as described in the text. Abscissa: distance in Angstrom from the boundary between solution phase and n-layer. Parameters on the curves give $N_+/2c$

Table 1. *Donnan-potential* ψ_D, *potential drop* $(\psi_\infty - \psi_0)$ *within the n-layer, and distance* d *of potential rise within the n-layer to less than* $1/e$ *from the asymptotic value for different ratios* $N_+/2c$ *of the concentration of fixed charges in the n-layer to concentration* c *in the electrolyte reservoir*

$N_+/2c$	1	2	5	10
ψ_0[mV]	22.3	36.5	58.4	75.7
$\psi_\infty - \psi_0$[mV]	10.5	15.6	20.7	22.9
d[A]	3.8	3.0	2.0	1.5

Here again, activity coefficient and partition coefficient of one and the presence of only one 1:1 univalent electrolyte, such as KCl, were used.

Our psn-model exhibits a transition region which is almost completely depleted of mobile ions. It consists of the s-layer and of small parts of the p- and n-layers adjacent to the s-layer. In these small depletion regions of the p- and n-layers, the space-charge density is high. Thus, a large junction potential exists across the s-layer, which will be characterized quantitatively in the following section. In the p- and n-layers outside the depletion regions, there are much higher total concentrations of mobile ions as compared to those in all other regions of the membrane. Thus, any applied bias voltage will appear almost completely across the small depletion regions of the p- and n-layers and the s-layer, whereas the regions of the p- and n-layers outside the depletion layers are regions of low field strength. Consequently, there the current densities can be obtained from the Nernst-Planck equations by neglecting the term in the field strength. In order to obtain the concentration gradients across the p- and n-layers, the following

two assumptions are made by the semianalytic approximation of Coster (1965).

(2) Even if a current flows, the ratio of the concentration of ions in the n-layer at the boundary to its depletion region to that in the p-layer at the boundary to its depletion region is still given by the Boltzmann distribution, using the total potential drop across the depletion layers in the n- and p-layers and the s-layer.

(3) After changing by an applied bias the equilibrium potential of a certain ion species across the central depletion region of the psn-junction as discussed above, only the concentration of the minority carriers rather than the majority carriers changes according to the Boltzmann distribution. This can be justified by the argument that it minimizes the space-charge density of the system.

(4) The space-charge regions of the depletion layers in the n- and p-layers are approximated as sharp rectangular distributions of uncompensated fixed charges.

These assumptions (1)–(4) of the semianalytic approximation have been checked by numerical integration of the Nernst-Planck equations for the abrupt pn-junction (Coster *et al.*, 1969). There it was shown that the ionic current and the electrical capacity can be calculated to an excellent approximation by the semianalytic method if the total width of the pn-junction is not too small. If the width of the two fixed-charge regions is chosen smaller than 2×35 A, there are certain deviations, especially with respect to assumptions (2) and (3). The reason for the deviations is that the width of the depletion layers becomes comparable to the total width of the pn-junction. Nevertheless, the current-voltage relation for membrane potentials > -350 V is predicted correctly by the semianalytic procedure, even down to a junction width of 2×25 A. In the case of the psn-junction, the above difficulty does not occur. As will be shown later, the effect of the s-layer is such that the depletion layers of the n- and p-layers are always completely negligible in width compared to the p- and n-layers. Thus, the semianalytic approximations seems to apply even better for the psn-junction than for the abrupt pn-junction.

A quantitative estimate, as to the conditions to be required, if assumption (2) is to hold, will be given in a later section. This estimate, too, confirms the applicability of assumption (2) of the semianalytic approximation. Thus, we can confidently expect this procedure to apply for the derivation of the steady state electrical properties of the psn-junction.

Electrical Capacity

We next wish to calculate the profile of electrical potential between the n- and p-layers.

The potential ψ is distributed according to the Poisson equation:

$$\frac{d^2\psi}{dx^2}=-\frac{\rho}{\varepsilon} \tag{3}$$

where ρ is the total charge density and ε the dielectric constant of the region in consideration. The direction x is normal to the membrane surface, the origin being the middle of the s-layer, which accordingly extends from $-l$ to $+l$ (*see* Fig. 1). According to our model, the charge density in the s-layer can be neglected. Thus we have:

$$\frac{d^2\psi}{dx^2}=0 \quad \text{for } -l\leqq x\leqq +l. \tag{4}$$

The general solution of Eq. (4) is:

$$\psi_s(x)=\alpha x+\beta \tag{5}$$

where α and β are constants to be assigned by the boundary conditions as follows. Because of the symmetry of our system we have:

$$\psi_s=0 \quad \text{at} \quad x=0, \quad \text{i.e.} \quad \beta=0. \tag{6}$$

In the depletion region of the n-layer, i.e., in the region $-l>x>-(l+\lambda)$, where $\lambda>0$ is the width of the depletion layer, we have according to assumption (4) of the semianalytic approximation:

$$-l>x>-(l+\lambda): \frac{d^2\psi}{dx^2}=-\frac{FN_+}{\varepsilon_n} \tag{7}$$

where F is the Faraday constant.

The general integral of Eq. (7) is:

$$\psi_n=-\frac{FN_+}{\varepsilon_n}\left(\frac{x^2}{2}+bx+c\right) \tag{8}$$

or

$$E_n(x)=\frac{d\psi_n}{dx}=-\frac{FN_+}{\varepsilon_n}(x+b). \tag{9}$$

Outside the depletion region, we have vanishing field strength in the n-layer, i.e.,

$$E_n=0 \quad \text{at} \quad x=-(l+\lambda) \tag{10}$$

or with Eq. (9):

$$b=l+\lambda. \tag{11}$$

At $x=-l$, we use continuity of the dielectric displacement:

$$\varepsilon_n E_n(-l)=\varepsilon_s E_s(-l). \tag{12}$$

Since $E_s(-l)=d\psi_s/dx=\alpha$, we get from Eqs. (9), (11) and (12):

$$\alpha=-\frac{FN_+}{\varepsilon_s}. \tag{13}$$

At $x=-l$, the electrical potential has to be continuous too; i.e., from Eqs. (5), (6), (8) and (13), we have:

$$c=\frac{l^2}{2}+\lambda l\left(1-\frac{\varepsilon_n}{\varepsilon_s}\right). \tag{14}$$

Thus, the complete course of electrical potential in the s-layer is:

$$-l\leqq x\leqq+l: \psi_s(x)=-\frac{FN_+}{\varepsilon_s}\lambda x. \tag{15}$$

In the depletion region of the n-layer we have:

$$-(l+\lambda)\leqq x\leqq l: \psi_n(x)=-\frac{FN_+}{\varepsilon_n}\left[\frac{x^2}{2}+(l+\lambda)x+\frac{l^2}{2}+\lambda l\left(1-\frac{\varepsilon_n}{\varepsilon_s}\right)\right]. \tag{16}$$

An analogous expression can be derived for the depletion region of the p-layer.

The total drop in electrical potential between the steady levels in the n- and p-layers is:

$$\psi_j=2\psi_n(-l-\lambda)=\frac{2FN}{\varepsilon}\left[\frac{\lambda^2}{2}+\lambda l\frac{\varepsilon}{\varepsilon_s}\right]. \tag{17}$$

Here we have used Eqs. (1), (2) and (16).

Similar to the case treated by Mauro (1962), the space-charge regions next to the s-layer represent a charged capacity. If we change by an applied bias the width of the depletion layers by $d\lambda$, the charge Q of the capacity

will be altered by:

$$dQ = FN\, d\lambda. \tag{18}$$

The differential electrical capacity C is then given by:

$$C = \frac{dQ}{d\psi_j}. \tag{19}$$

From Eq. (17) we obtain:

$$\frac{d\psi_j}{d\lambda} = \frac{2FN}{\varepsilon}\left[\lambda + l\frac{\varepsilon}{\varepsilon_s}\right]. \tag{20}$$

Thus, from Eqs. (18)–(20), we have finally

$$C = \frac{\varepsilon_s}{2l\left(1+\frac{\varepsilon_s}{\varepsilon}\frac{\lambda}{l}\right)}. \tag{21}$$

To discuss Eq. (21), we first notice the dependence of λ on ψ_j, i.e., on the membrane potential. According to Eq. (17), we get:

$$\lambda = \frac{l\varepsilon}{\varepsilon_s}\left[\left(1+\frac{\psi_j \varepsilon_s^2}{FN l^2 \varepsilon}\right)^{\frac{1}{2}} - 1\right]. \tag{22}$$

For an estimate of the order of magnitude of the terms in Eq. (22), we set: $N = 2$ M, $\varepsilon_s = 4\,\varepsilon_0$, $\varepsilon = 40\,\varepsilon_0$, $l = 2 \cdot 10^{-7}$ cm. Using the Donnan potential ψ_D for $N = 2$ M from Table 1 and for the resting potential of the squid giant axons $|V_r| = 60$ mV, we have:

$$\psi_j = 2\psi_D + |V_r| = 132 \text{ mV}.$$

Since

$$\frac{\psi_j \varepsilon_s^2}{FN l^2 \varepsilon} = 6.06 \cdot 10^{-4} \ll 1 \tag{23}$$

we obtain in an excellent approximation from Eq. (22):

$$\frac{\lambda}{l} = \frac{\psi_j \varepsilon_s}{2FN l^2}. \tag{24}$$

Using again the parameters given above, we get:

$$\lambda/l = 3.03 \cdot 10^{-3}. \tag{25}$$

Any other reasonable choice of parameters would give the same picture. Thus, in contrast to the abrupt pn-junction, the width of the depletion regions is indeed very small compared to that of the p- and n-layers, as stated in the discussion of the semianalytic procedure. Using Eqs. (21) and (25), we have in a very good approximation:

$$C=\frac{\varepsilon_s}{2l}. \tag{26}$$

With the numbers $l=2\cdot 10^{-7}$ cm and $\varepsilon_s=4\,\varepsilon_0$, we obtain:

$$C=0.9\cdot 10^{-6}\ \text{Farad cm}^{-2} \tag{27}$$

as observed for the squid giant axon (Cole & Moore, 1960) and, indeed, for many other biological membranes (Cole, 1965). To check the dependence of the differential capacity on the membrane potential, we use Eqs. (21) and (24). For 100-mV de- or hyperpolarization, the relative deviation of C from the resting value is less than 0.001. This compares well with the insensitivity of the electrical capacity of the squid giant axon membrane on the membrane potential as shown by Cole (1969, p. 136). The independence of the electrical capacity of the psn-junction on membrane potential, as derived above, is not found for the abrupt pn-junction. Coster *et al.* (1969) have demonstrated a strong dependence of the capacity on membrane potential. Using $N_+=N_-=2$ M for the abrupt pn-junction and a resting potential of 60 mV, we calculate with their procedure for 100-mV depolarization a capacity 2.03 times the resting capacity, whereas 100-mV hyperpolarization gives 0.75 times the resting capacity.

In passing, we mention that the "punch-through effect", discussed by Coster (1965) and Coster *et al.* (1969), occurs for the psn-junction at much higher membrane potentials than for the abrupt pn-junction. Punch-through, as defined by Coster (1965), should occur if a depletion region extends all through the fixed-charge lattice. If we use $N=2$ M, $\varepsilon=40\,\varepsilon_0$, $\varepsilon_s=4\,\varepsilon_0$, $l=20$ A, and $\lambda=30$ A, we obtain for the punch-through potential $\bar{\psi}_j$ from Eq. (17):

$$\bar{\psi}_j=70\ V. \tag{28}$$

This means punch-through does practically not occur in the psn-model. Its calculated range is two to three orders of magnitude larger than the electrical breakdown observed for biological membranes (Coster, 1965).

In conclusion, the main result of this section is contained in Eq. (26), which shows the membrane capacity of the psn-junction to be practically independent of the fixed-charge density and the membrane potential.

Ionic Fluxes Through the Membrane

For reference, first we cite data on ionic concentrations of freshly isolated squid axons (*Loligo*), given by Hodgkin (1964, p. 28):

Axoplasm: 400 mM K^+, 50 mM Na^+, 108 mM Cl^-, 0.4 mM Ca^{++}, 10 mM Mg^{++}, 250 mM isethionate.

Blood: 20 mM K^+, 440 mM Na^+, 560 mM Cl^-, 10 mM Ca^{++}, 54 mM Mg^{++}.

The value for the axoplasmic Cl^- concentration was taken from the extensive investigation on this point of Keynes (1963). The axonal resting potential of *Loligo in vivo* is approximately -60 mV inside negative (Moore & Cole, 1960). From experiments with radioactive tracers, it is known that the fluxes of the divalent cations Ca^{++} and Mg^{++} through the membrane are negligible compared to those of the univalent ions (Hodgkin & Keynes, 1957; Tasaki, Watanabe & Lerman, 1967; Tasaki & Singer, 1967). Data on the flux of isethionate are not known to the author; in the following, we shall neglect its eventual permeation through the membrane as well. Data on the fluxes of K^+, Na^+ and Cl^- through giant axons of squid are abundant in the literature. These ions are the major contributors to the ionic fluxes the squid axon membrane and only these will be considered in this section.

Data on Na^+ fluxes for the giant axon of *Dosidicus* have been published by Canessa-Fischer, Zambrano and Rojas (1968). The K^+ and Na^+ fluxes for *Sepia* have been investigated in detail by Keynes (1951) and Hodgkin and Keynes (1955). Data on *Loligo pealeii* have been given by Shanes and Berman (1955) and Brinley and Mullins (1965). Data on K^+, Na^+, and Cl^- fluxes for *Loligo forbesi* were obtained by Caldwell, Hodgkin, Keynes and Shaw (1960), Caldwell and Keynes (1960), and Keynes (1963).

The variation of univalent ion fluxes between the different species are within the variations of the results of different authors on the same species. Thus, it can be said generally that the influx and the efflux of each ion roughly compensate each other, and that furthermore the in- and effluxes of K^+ and Na^+ are about 50 pmoles/cm^2 sec, whereas the Cl^- in- and efflux are about half of that. Tasaki (1963) and Tasaki and Singer (1967), for somewhat different conditions (internally perfused axons), report somewhat higher numbers for the K^+ and Na^+ fluxes. In the following, we shall use the data on *Loligo forbesi* given by Caldwell *et al.* (1960), Caldwell and Keynes (1960) and Keynes (1963), because these are the most complete. For reference they are assembled in Table 2. The Na^+ efflux given there is the mean for 42 unpoisoned axons, calculated from columns 9 and 11 of Tables 3 and 4 of Caldwell *et al.* (1960); its passive component is the mean for 44 poisoned axons, calculated from columns 6, 7 and 11 of these tables.

Table 2. *Total and passive components of ion fluxes for* Loligo forbesi

Flux	K^+_{tot}	K^+_{pass}	Na^+_{tot}	Na^+_{pass}	Cl^-_{tot}	Cl^-_{pass}
Influx [pmole/cm^2 sec]	19[a]	$\sim 5-10$[a]	42[a]	~ 42[a]	22.8[b]	~ 9[b]
Efflux [pmole/cm^2 sec]	38[c]	~ 38[a,c]	70.4[d]	~ 11[e]	20.8[b]	~ 20[b]

[a] Caldwell *et al.* (1960).
[b] Keynes (1963).
[c] Caldwell and Keynes (1960).
[d] Computed from columns 9 and 11 of Tables 3 and 4 in reference a.
[e] Computed from columns 6, 7 and 11 of Tables 3 and 4 in reference a.

The nature of the univalent ion fluxes has been elucidated by the study of the influence of metabolic inhibitors. For axons from *Sepia* and *Loligo forbesi*, Hodgkin and Keynes (1955) and Caldwell *et al.* (1960) have shown that the metabolic inhibitors cyanide or 2,4-dinitrophenol (DNP) reduce the efflux of Na^+ to about 1/10 its normal value, whereas the influx of Na^+ is essentially unaffected. Lowering the temperature to about 1 °C also inhibits the Na^+ efflux but hardly affects the Na^+ influx. One can conclude that the Na^+ efflux is driven largely by a metabolic ion pump, whereas the Na^+ influx is passive.

Similarly, Caldwell *et al.* (1960) could show that cyanide poisoning reduces the K^+ influx into *Loligo* axons to between 25 and 50% its normal value of 19 pmoles/cm^2 sec, the K^+ efflux being unaffected by cyanide. Thus, the metabolically independent (i.e., passive) component of the K^+ influx is between 5 and 10 pmoles/cm^2 sec.

The Cl^- influx also is partly dependent on energy metabolism. Keynes (1963) showed that about 50% of Cl^- influx into axons of *Loligo forbesi* is inhibited by 2,4-DNP or cyanide, whereas the Cl^- efflux is unaffected by the inhibitors. We can take the metabolically independent components of the ion fluxes as the passive fluxes. The passive components of the ion fluxes, as obtained from inhibitor studies, are given in Table 2.

In the following, we wish to describe the net passive ion fluxes in the resting state in terms of our model. In the resting state, we assume electroneutrality of total fluxes, and furthermore time independence of ionic concentrations in the inside and outside reservoirs. Thus, the total influx of an ion should cancel its efflux in the resting state. For Cl^-, the data in Table 2 are in agreement with this assumption. In the cases of Na^+ and K^+, the equality of fluxes is only given by order of magnitude. In addition to variations of the biological material in general, the following causes may contribute to the deviations between in- and effluxes of Na^+ and K^+. The concentrations of high-energy phosphates in the axoplasm might have been changed or depleted. The state of maintenance of the membrane-bound Na^+-K^+-ATPase might have been changed with respect to its metabolic rate and its degree of coupling between Na^+ and K^+ transport. The passive permeabilities might have changed in the preparation. The ionic concentration gradients, which are maintained carefully *in vivo*, might have changed in the *in vitro* preparation at the time of measurement. We feel that most of these changes are more severe for the metabolic ion pump. For instance, changes in the concentrations of minority cations in the external and internal media should affect the metabolic ion pump strongly, but affect less strongly the passive permeability. Thus, we consider the passive components of the ions fluxes as discerned by the inhibitor studies to be more reliable and to represent the passive fluxes of the resting axon.

Net Passive Ion Flux in the psn-Model

In this section, we use an activity coefficient of one; i.e. we use concentrations instead of chemical activities. For each ionic species l, we can calculate the membrane potential V_l for which there is no net passive flux, the "equilibrium potential", from the inside ionic concentration c_l'' and the outside concentration c_l':

$$V_l = -\frac{RT}{zF} \ln \frac{c_l''}{c_l'} \tag{29}$$

where $z=+1$ for Na^+ and K^+, and -1 for Cl^-. From the measured ionic concentrations, reproduced above, we obtain at $T=20$ °C:

$$V_K=-76\,\text{mV}; \quad V_{Na}=55\,\text{mV}; \quad V_{Cl}=-42\,\text{mV}. \tag{30}$$

Thus, at the resting potential $V_r=-60$ mV, there will be a net passive flux for each of the ion species considered. In order to calculate these fluxes in the semianalytic approximation discussed above, we have to observe that only the minority ions contribute appreciably to the total ionic flux (Coster, 1965). Since the electric field is essentially zero in the fixed-charge layers, we can calculate the flux Φ_l of the ion species l as resulting from pure diffusion in that layer, where it is minority mobile ion. Thus, according to Eq. (14) from Coster (1965) we can write:

$$\Phi_l=\frac{D_l}{W_l}(c_{lj}-c_{l0}). \tag{31}$$

Here, D_l is the diffusion coefficient of cation species l in the n-layer, or of an anion species l in the p-layer. Similarly, c_{l0} is the concentration of cation species l at the outside face of the n-layer, where the Donnan potential has just attained the potential level inside the n-layer, wereas c_{lj} is the cation concentration of species l at the boundary between depletion region and the bulk of the n-layer. For an anionic species l, c_{lj} and c_{l0} are the corresponding quantitites for the p-layer. For a cation l, W_l is the width of the n-layer minus the depletion layer, whereas for an anion it is the width of the p-layer minus its depletion layer. In contrast to the corresponding parameters W_{N^+} and W_{N^-} used by Coster (1965) for the abrupt pn-junction, our W_l parameters are independent of the membrane potential and practically equal to the width of the n- or p-layer as shown above. Because of the symmetry of our model we can thus write:

$$W_l=L \tag{32}$$

where L is the width of the fixed-charge layers. In this discussion, we have neglected the voltage-independent widths of the transition regions between fixed-charge layers and inside or outside medium. As was shown above, they are small compared to the total widths of the fixed-charge layers and do not change for fixed ionic concentrations inside and outside, as discussed in this paper.

We now have to express the concentrations c_{l0} and c_{lj} by the concentrations in the inside and outside medium and by the membrane potential.

When considering the equilibrium distribution of ionic species between electrolyte reservoir and fixed-charge layer where it is the minority ion, it is convenient to introduce the partition coefficient k_l as follows:

$$k_l = \frac{c_{l0}}{c_l} \exp\left\{\frac{FV_{Dl}}{zkT}\right\}. \tag{33}$$

By the use of this equation, it is possible to express the concentration c_{l0} of cation species l in the n-layer at its equilibrium potential by the partition coefficient k_l, its concentration c_l in the outside medium and the Donnan potential V_{Dl}, between outside medium and n-layer, where, of course, V_{Dl} is the same for all ions distributed between outside medium and n-layer. Similarly, the concentration of an anionic species l in the p-layer at its equilibrium potential can be expressed, with use of Eq. (33), by its concentration c_l in the inside medium, its partition coefficient k_l between electrolyte and p-layer and the Donnan potential V_{Dl} at the inside face of the p-layer. At the equilibrium potential V_l, similar partition equilibria are valid between all the layers of the composite psn-membrane.

The situation is different at any membrane potential V which is different from the equilibrium potential. Then, according to the semianalytic approximation, Eq. (33) remains valid only at the boundary between the inside or outside electrolyte reservoir and the corresponding fixed-charge lattice (Coster, 1965). Since, in the semianalytic approximation, the applied bias voltage occurs only across the depletion layers and the s-layer, and since the minority carriers at the boundary between the depletion layer and the rest of the fixed-charge layer in this approximation are distributed according to the Boltzmann factor, we have:

$$c_{lj} = c_{l0} \exp\left\{\frac{F(V-V_l)}{RT}\right\}. \tag{34}$$

Here V is the membrane potential and $(V-V_l)>0$ for a depolarizing displacement from the equilibrium potential. Using Eqs. (31)–(34), we can write for the flux Φ_l:

$$\Phi_l = P_l c_l \left[\exp\left\{\frac{F(V-V_l)}{RT}\right\} - 1\right] \tag{35}$$

where the permeability P_l is given by:

$$P_l = \frac{k_l D_l}{L} \exp\left\{-\frac{FV_{Dl}}{RT}\right\}. \tag{36}$$

We can assign numerical values to the permeabilities P_l, if we put $V_r = -60$ mV (resting potential) in Eq. (35) and use the experimentally deter mined net passive fluxes and ionic concentrations.

From Table 2 we have for the net passive ion fluxes in pmoles/cm^2 sec

$$\Phi_K = 28 \text{ to } 33 \approx 30; \quad \Phi_{Na} = 31; \quad \Phi_{Cl} = 12. \tag{37}$$

The K^+ and Cl^- fluxes are outward; the Na^+ flux is inward. Using for c the numbers:

$$c'_K = 0.020 \text{ M}; \quad c'_{Na} = 0.440 \text{ M}; \quad c''_{Cl} = 0.108 \text{ M} \tag{38}$$

and Eq. (30), we obtain:

$$P_K = 1.70 \cdot 10^{-6} \frac{\text{cm}}{\text{sec}}; \quad P_{Na} = 7.12 \cdot 10^{-8} \frac{\text{cm}}{\text{sec}}; \quad P_{Cl} = 2.18 \cdot 10^{-7} \frac{\text{cm}}{\text{sec}}. \tag{39}$$

The permeability ratios

$$P_K : P_{Na} : P_{Cl} = 1 : 0.042 : 0.128 \tag{40}$$

turn out to be very similar to those derived by the constant field procedure for K and Na (Hodgkin & Katz, 1949) and for K and Cl (Keynes, 1963).

At this place, we can give an estimate on the order of magnitude of the K^+ permeability in the s-layer, which is necessary for the semianalytic approximation in the form of Eq. (34) to be valid. The Nernst-Planck equation for K^+ in the s-layer reads:

$$\Phi_{Ks} = -D_{Ks}\left(\frac{dc_K}{dx} + \frac{Fc_K}{RT}\frac{d\psi}{dx}\right). \tag{41}$$

Here, D_{Ks} is the diffusion coefficient in the s-layer and c_K the concentration in the s-layer.

For the Boltzmann relation (34) to be valid, each of the two terms on the right side of Eq. (41) must be large compared to the flux Φ_{Ks}. The flux Φ_{Ks}, of course, must be equal to the net passive flux $\Phi_K = 30$ pmoles/cm^2 sec. Thus, the following inequality should be fulfilled.

$$\left| D_{Ks}\frac{dc_K}{dx} \right| \gg \Phi_K = 30 \text{ pmoles/cm}^2 \text{ sec}. \tag{42}$$

The concentration gradient dc_K/dx can be approximated by the concentration difference between the p-layer and the boundary between depletion layer and n-layer divided by total thickness $2 \cdot l$ of the s-layer if a partition coefficient of one is used between the s- and p-layer. The cation concentration between the depletion layer and the n-layer can be neglected compared to that in the p-layer. The K^+-concentration in the p-layer is given

by a relation similar to Eq. (33):

$$c_{Kp}=k_p c_K'' \exp\left\{\frac{FV_{Dp}}{RT}\right\} \tag{43}$$

where k_p is the partition coefficient for K^+ between the inside medium and the p-layer, c_K'' is the K^+ concentration in the inside medium, and $V_{Dp}>0$ is the Donnan potential between the inside medium and the p-layer. For the numerical estimate, we use $k_p=1$, $c_K''=0.5$ M, $N_+=2$ M; i.e., $V_{Dp}=36$ mV, and $2\cdot l=40$ A.

Thus,

$$\frac{dc_K}{dx}\approx\frac{c_{Kp}}{2\cdot l}\approx 5\cdot 10^3 \text{ moles}\cdot\text{cm}^{-4} \tag{44}$$

and

$$D_{Ks}\gg\Phi_K\Big/\frac{dc_K}{dx}\approx 6\cdot 10^{-14}\frac{\text{cm}^2}{\text{sec}}. \tag{45}$$

From the value $P_K=1.70\cdot 10^{-6}$ cm/sec, obtained above for the n-layer, we can estimate from Eq. (36)

$$D_K\approx 2\cdot 10^{-12}\text{ cm}^2/\text{sec} \tag{46}$$

where we have used again $V_{Dl}=36$ mV, $k_l=1$ and $L=30$ A. Thus, for Eqs. (45) and (46) to be fulfilled, we have to require that $D_{Ks}\geqq D_k$. This is equivalent to stating that the major permeability barriers to ion flow of our composite membrane are those regions where the ion species considered is the minority mobile ion.

For the above estimate, only the relative magnitudes of D_K and D_{Ks} are of interest. The absolute magnitudes of these quantities, of course, depend on the choices of the partition coefficients and the fixed-charge densities, which are not known *a priori.*

Total Electric Current Through the Membrane

In the steady state of axoplasmic ion concentrations, as assumed for the resting state, the net passive ion fluxes are balanced by equal but opposite ion fluxes which are driven metabolically. These active fluxes can be assumed to be independent of the membrane potential. For Na^+ extrusion from squid giant axons, this was shown to be true by Hodgkin and Keynes (1955) and by Brinley and Mullins (1970). Because of the coupling between Na^+ extrusion and the metabolically driven K^+ uptake, we can presume potential independence for the latter too. For the active part of the Cl^- uptake, explicit data of this kind are not available. The contribution of Cl^- to the total electric current will turn out to be very small, however, so that the assumption of potential independence of all active ionic fluxes seems to be reliable for the results of the following calculations.

The passive electric current $I_{pass}(V)$ is the sum of the individual ioni currents given by Eq. (35) multiplied by the Faraday constant:

$$I_{pass}(V)=F\sum_l P_l c_l\left[\exp\left\{\frac{F(V-V_l)}{RT}\right\}-1\right]. \tag{4}$$

Here, the direction of the ionic fluxes Φ_l was considered so as to take a outward flux of positive charge as a positive current. The active current I_a can be expressed by Eq. (47) taken at the resting potential V_r:

$$I_{act}=-I_{pass}(V_r). \tag{4}$$

Thus, the total electric current $I(V)$ can be written:

$$I(V)=F\left[\exp\left\{\frac{FV}{RT}\right\}-\exp\left\{\frac{FV_r}{RT}\right\}\right]\sum_l P_l c_l \exp\left\{-\frac{FV_l}{RT}\right\}. \tag{49}$$

From Eq. (49) we can compute the membrane resistance R as:

$$1/R=\frac{dI(V)}{dV}=\frac{F^2}{RT}\exp\left\{\frac{FV}{RT}\right\}\sum_l P_l c_l \exp\left\{-\frac{FV_l}{RT}\right\}. \tag{5C}$$

At the resting potential $V_r=-60$ mV, we get with the numbers in Eqs. (30) (38) and (39):

$$R=3.45\cdot 10^3\ \Omega\,\mathrm{cm}^2. \tag{51}$$

This number, which was computed from data of the chemical ion fluxes can be compared with the electrically measured value. It turns out to b in the magnitude observed experimentally. Cole and Moore (1960), fo instance, have obtained a resting resistance of $1.4\cdot 10^3\ \Omega\,\mathrm{cm}^2$. By applicatio of the constant-field procedure (*see*, for instance, Keynes, 1951), on obtains the very similar value of $R=3.25\cdot 10^3\ \Omega\,\mathrm{cm}^2$ for the electrica resistance, if again the data compiled in Table 2 are used.

Even without a voltage dependence of the ionic permeabilities, th electrical current of the psn-model, given in Eq. (49), exhibits rectification It is of interest to compare this theoretical steady state current-voltag characteristic with the experimental one. Since we are interested in th current-voltage relation near the resting state, we use the data measure directly by a voltage clamp technique and given by Cole and Moore (1960) In Fig. 3 we have plotted the experimental curve from Fig. 17 of thes authors for comparison with the theoretical curve according to Eq. (49

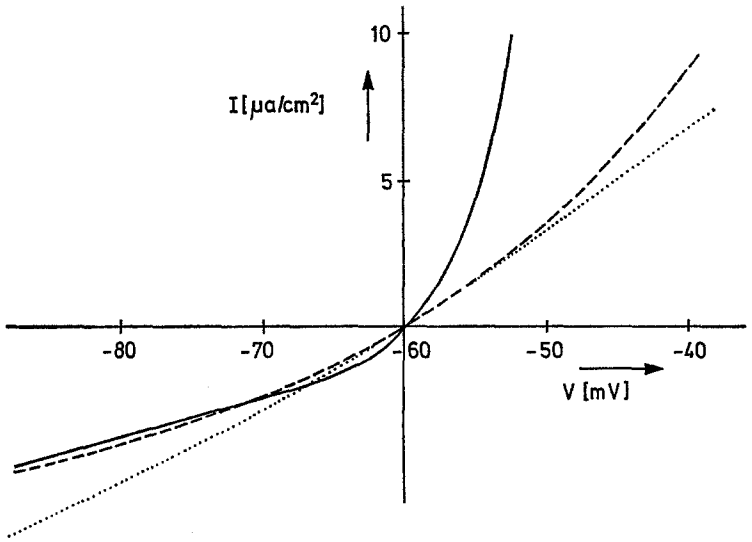

Fig. 3. Plot of steady state electric current I vs. membrane potential V for squid giant axon near the resting potential of -60 mV. Fully drawn is the experimental curve, taken from Fig. 17 of Cole and Moore (1960); broken curve is calculated from tracer fluxes according to Eq. (49) of the text; dotted curve is computed from tracer fluxes according to the constant-field procedure

using the chemical data of Eqs. (30), (38) and (39). We have plotted also the characteristic following from the constant-field procedure, using the same chemical data. As can be seen from this figure, the psn-model gives a stronger rectification than the constant-field assumption, but does not suffice to reproduce the experimental results without invoking a potential dependence of the ionic permeabilities. In an earlier paper (Adam, 1970), we have given the description of a cooperatively occurring transition of the axon membrane which takes place at and slightly above the resting potential. Concurrently with this change of the state of the membrane, the ionic permeabilities change and give rise to a strongly voltage-dependent passive conductance (Adam, 1970). It is to this additional feature of the axon membrane that we wish to ascribe the marked deviations between the experimental and the theoretical curve in Fig. 3 at depolarizing potentials. A more detailed theoretical description of this additional feature of a cooperative change in the steady state of the membrane and its concomitant change in passive ionic permeability will be published elsewhere.

Discussion

As shown in the sections above, the ionic psn-model proposed for the resting axon membrane accounts well for the observed steady state electrical

characteristics. From a theoretical description of the kinetic processe during axon excitation (Adam, 1967, 1968, 1970), there are further argument in favor of an ionic psn-structure of the axon membrane. Thus, it seem very promising to try to prove or disprove by the methods of protei chemistry the presence of the proposed asymmetry in the actual membrane

The direct isolation and characterization of axonal membrane protein seems to be fairly difficult because of the unavoidable contaminatio by membrane proteins from the surrounding Schwann cell layer. Fron the work of Camejo, Villegas, Barnola and Villegas (1969), however, i appears possible to distinguish between different membrane fractions, s that one can hope this approach will become fruitful.

Another possibility for an experimental test seems to be the sequentia treatment of the membrane with trypsin and a carboxypeptidase in orde to remove positively charged amino acids from the axonal membran proteins and then to test for cation transport or electrical conductivity

Also the method of selective reaction of membrane-bound amino group with 1-fluoro-2,4-dinitrobenzene seems to be an interesting test. In a preliminary account, Strickholm, Clark and Shrager (1970) report on th action of such reagents on crayfish ventral nerve. As predicted from ou model, the ratio of K^+ to Cl^- permeability increases by this treatment

Clearly, more experiments of this kind are necessary to prove or disprov the psn-model.

If indeed the nature of ion permeability control turns out to be tha envisioned above, then the hitherto poorly defined structural protein of th plasma membrane might prove to be functionally important. Then, th charged groups of membrane structural proteins would control the intra- cellular ionic content and the membrane potential, i.e., the very basi of life processes in the cell.

I wish to thank Professors Max Delbrück (Pasadena, Calif.) and Peter Läuge (Konstanz, Germany) for valuable critical discussions.

The support of part of the present work by a Habilitandenstipendium of the Deutsch Forschungsgemeinschaft is gratefully acknowledged.

References

Adam, G. 1967. Nervenerregung als kooperativer Kationenaustausch in einem zwei- dimensionalen Gitter. *Ber. Bunsenges* **71**:829.

— 1968. Theorie der Nervenerregung als kooperativer Kationenaustausch in einem zweidimensionalen Gitter. I. Ionenstrom nach einem depolarisierenden Sprung im Membranpotential. *Z. Naturf.* **23b**:181.

Adam, G. 1970. Theory of nerve excitation as a cooperative cation exchange in a two-dimensional lattice. *In:* Physical Principles of Biological Membranes. F. Snell, J. Wolken, G. Iverson, J. Lam, editors. p. 53. Gordon and Breach Science Publishers, New York.

Brinley, F. J., Jr., Mullins, L. J. 1965. Ion fluxes and transference number in squid axons. *J. Neurophysiol.* **28**:526.

– – 1970. The effect of membrane potential and internal potassium on sodium efflux from dialyzed squid giant axons. 14th Ann. Meeting Biophys. Soc., Feb. 25–27, 1970. Abstr. WPM-A 6.

Caldwell, P. C., Hodgkin, A. L., Keynes, R. D., Shaw, T. I. 1960. The effects of injecting energy rich phosphate compounds on the active transport of ions in the giant axon on *Loligo*. *J. Physiol.* **152**:561.

– Keynes, R. D. 1960. The permeability of the squid giant axon to radioactive potassium and chloride ions. *J. Physiol.* **154**:177.

Camejo, G., Villegas, G. M., Barnola, F. V., Villegas, R. 1969. Characterization of two different membrane fractions isolated from the first stellar nerves of the squid *Dosidicus gigas*. *Biochim. Biophys. Acta* **193**:247.

Canessa-Fischer, M., Zembrano, F., Rojas, E. 1968. The loss and recovery of the sodium pump in perfused squid axon. *J. Gen. Physiol.* **51**:162*s*.

Cole, K. S. 1965. Theory, experiment, and the nerve impulse. *In:* Theoretical and Mathematical Biology. T. H. Waterman, H. J. Morowitz, editors. p. 136. Blaisdell Publ. Co., New York.

– 1968. Membranes, Ions and Impulses. University of California Press, Berkeley.

– Moore, J. W. 1960. Ionic current measurements in the squid giant axon membrane. *J. Gen. Physiol.* **44**:123.

Coster, H. G. L. 1965. A quantitative analysis of the voltage current relationships of fixed charge membranes and the associated property of "punch-through". *Biophys. J.* **5**:669.

– George, E. P., Simons, R. 1969. The electrical characteristics of fixed charge membranes: Solution of the field equations. *Biophys. J.* **9**:666.

Davson, H., Danielli, J. F. 1952. The Permeability of Natural Membranes. University Press, Cambridge.

Dickerson, R. E., Kopka, M. L., Weinzierl, J., Varnum, J., Eisenberg, D., Margoliash, E. 1967. Localization of the heme in horse heart ferricytochrome C by X-ray diffraction. *J. Biol. Chem.* **242**:3015.

Herlet, A., Spenke, E. 1955. Gleichrichter mit pin- beziehungsweise psn-Struktur unter Gleichstrombelastung. *Z. Angew. Physik* **7**:99, 149, 195.

Hodgkin, A. L. 1964. The Conduction of the Nervous Impulse. p. 28. University Press, Liverpool.

– Keynes, R. D. 1955. Active transport of cations in giant axons from *Sepia* and *Loligo*. *J. Physiol.* **128**:28.

– – 1957. Movements of labelled calcium in squid giant axons. *J. Physiol.* **138**:253.

Karlson, P. 1966. Kurzes Lehrbuch der Biochemie. p. 34. Thieme Verlag, Stuttgart.

Keynes, R. D. 1951. The ionic movements during nervous activity. *J. Physiol.* **114**:119.

– 1963. Chloride in the squid giant axon. *J. Physiol.* **169**:690.

Margoliash, E. 1962. Amino acid sequence of chymotryptic peptides from horse heart cytochrome C. *J. Biol. Chem.* **237**:2161.

Mauro, A. 1962. Space charge regions in fixed charge membranes and the associated property of capacitance. *Biophys. J.* **2**:179.

Moore, J. W., Cole, K. S. 1960. Resting and action potentials of the squid giant axon *in vivo*. *J. Gen. Physiol.* **43**:961.

Mueller, P., Rudin, D. O. 1967. Action potential phenomena in experimental bimolecula lipid membranes. *Nature* **213**:603.

— — 1968*a*. Action potentials induced in bimolecular lipid membranes. *Natur* **217**:713.

— — 1968*b*. Resting and action potentials in experimental bimolecular lipid membranes *J. Theoret. Biol.* **18**:222.

Rice, S. A., Nagasawa, M. 1961. Polyelectrolyte Solutions. p. 470. Academic Press New York.

Shanes, A. M., Berman, M. D. 1955. Kinetics of ion movement in the squid giant axon *J. Gen. Physiol.* **39**:279.

Stoeckenius, W., Engelman, D. M. 1969. Current models for the structure of biologica membranes. *J. Cell Biol.* **42**:613.

Strickholm, A., Clark, H. R., Shrager, P. 1970. The dependence of membrane ionic permeability and excitation on amino groups. 14th Ann. Meeting Biophys. Soc. Feb. 25–27, 1970. Abstr. FAM-A6.

Tasaki, I. 1963. Permeability of squid axon membrane to various ions. *J. Gen. Physiol* **46**:755.

— Singer, I. 1966. Membrane macromolecules and nerve excitability: A physico-chemical interpretation of excitation in squid giant axons. *Ann. N.Y. Acad. Sci.* **137**:792.

— Watanabe, A., Lerman, L. 1967. Role of divalent cations in excitation of squid giant axons. *Amer. J. Physiol.* **213**:1465.

Villegas, G. M., Villegas, R. 1968. Ultrastructural studies of squid nerve fibers. *J. Gen. Physiol.* **51**:44*s*.